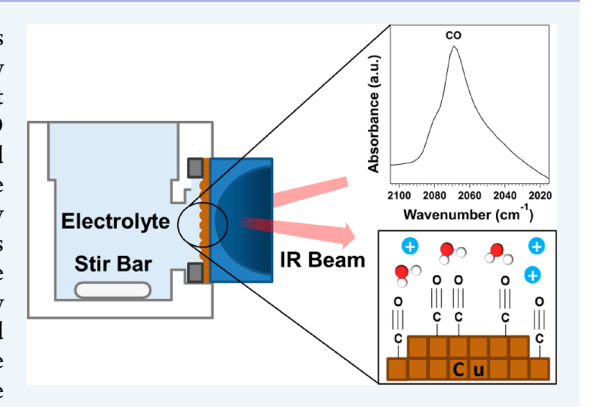


Impact of Forced Convection on Spectroscopic Observations of the Electrochemical CO Reduction Reaction

Arnav S. Malkani,[†] Jing Li,[‡] Jacob Anibal,[†] Qi Lu,*,[‡] and Bingjun Xu*,[†]

Supporting Information

ABSTRACT: The electrochemical CO reduction reaction (CORR) has been shown to suffer from mass transport limitations owing to the low solubility of CO in aqueous electrolytes (∼1 mM). However, no direct observation of the impact of the mass transport on the adsorbed CO coverage on Cu, and in turn the CORR activity, has been reported because of the lack of suitable experimental techniques. In this work, we employ operando surface enhanced infrared absorption spectroscopy with and without stirring to investigate the CO binding sites at potentials relevant to the CORR and correlate with reactivity studies. The significant loss in CO peak intensity observed in the spectra at below −0.6 V without stirring highlights the importance of including forced convection in spectroscopic studies to obtain information representative of typical reaction conditions. Despite roughly 1 order of magnitude lower CO coverage on Cu at −0.7 V without stirring, as compared to the



case with stirring, the relative distribution of CORR products does not change appreciably, suggesting that adsorbed CO on Cu exists in patches rather than distributing uniformly.

KEYWORDS: ATR-SEIRAS, CO reduction reaction, copper, electochemistry, forced convection, stirring, operando spectroscopy

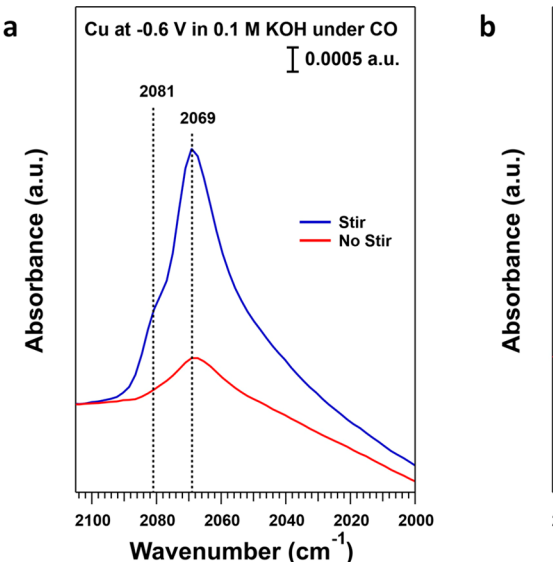
E lucidating the reaction mechanism of the electrochemical CO reduction reaction (CORR) on Cu is critical in the catalyst design for the renewable upgrading of CO2 because CO is a known intermediate in the electroreduction of CO2 to valuable hydrocarbons and oxygenates. 1,2 The CORR performed independently in alkaline environments favors the production of C-C coupling products (e.g., ethylene and ethanol); however, the low solubility of CO in aqueous solutions (~1 mM) could become a limiting factor.³ This was highlighted by the recent work which attributed a shoulder in the CVs on polycrystalline Cu at -0.65 V vs RHE in hydroxide to a CO mass transport limitation phenomenon.⁴ All potentials in this work will be referenced to the reversible hydrogen electrode (RHE) scale unless otherwise noted. It is important to understand the impact of mass transport of CO on the activity and product distribution in the CORR, and in this regard, spectroscopic results could provide key information on the CO surface coverage. Linearly bonded CO bands reported in infrared studies show a trend of increasing intensity with coverage which allows for a semiquantitative method to estimate CO surface coverage. 5-7 Surface enhanced infrared spectroscopy (SEIRAS) is a sensitive technique to probe electrochemical interfaces, ⁸⁻¹¹ although signal penetration depths may vary on the basis of the nature and thickness of the metal film. ^{12,13} In all cases, the spectra are dominated by species within the electrical double layer without much

influence from bulk species.¹⁴ However, conventional spectro-electrochemical cells for SEIRAS do not have the capability of stirring, thus limiting its application in understanding the effect of mass transport of CO on the reaction. Further, SEIRAS investigations of CORR in alkaline conditions, especially at the potential range commonly employed in reactivity studies (\leq -0.6 V), have been scarce. ^{15,16} This could be in part due to the instability of Cu films needed for this technique in the alkaline conditions and another impediment caused by the lack of forced convection in the spectroelectrochemical cells that is discussed in this work. Recently, we developed a custom-made stirring SEIRAS cell (Figure S1) to improve mass transport of reactants during spectroscopic investigations in a configuration that resembles a standard Hcell typically used for electrochemical measurements. 9,10 Previous spectroscopic work on electrochemical oxidation reactions have employed the use of flow cells as an alternate way to improve mass transport in spectroscopic studies. ^{17,18} In this work, we employ the SEIRAS stir cell to demonstrate the impact of stirring on CO coverage on Cu surfaces at potentials relevant to the CORR, highlighting the importance of forced convection in obtaining reliable spectroscopic information to

Received: August 22, 2019
Revised: November 17, 2019
Published: December 11, 2019

[†]Center for Catalytic Science and Technology, Department of Chemical and Biomolecular Engineering, University of Delaware, Newark, Delaware 19716, United States

[‡]State Key Laboratory of Chemical Engineering, Department of Chemical Engineering, Tsinghua University, 100084 Beijing, China



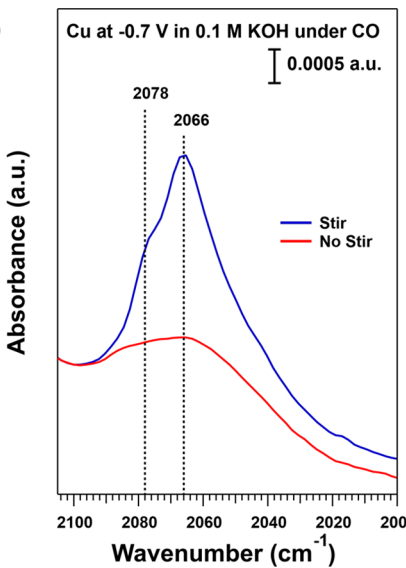


Figure 1. ATR-SEIRAS spectra in CO-saturated 0.1 M KOH showing the linearly bonded CO peak region on a chemically deposited polycrystalline Cu film when switching from stirring at 800 rpm to no stirring. Spectra presented correspond to 64 coadded scans collected with a 4 cm⁻¹ resolution. Background spectrum was taken at 0.1 V in argon-saturated electrolyte.

correlate with reactivity results. Further, we show that the relative selectivity for various CORR products is insensitive to the surface CO coverage, indicating adsorbed CO exists in patches rather than being uniformly distributed on the Cu surface.

Stirring has a drastic impact on the observed spectroscopic features of adsorbed CO on polycrystalline Cu surfaces at potentials relevant to the CORR, highlighting the importance of the forced convection in operando spectroscopy. Linearly adsorbed CO, referred to as CO_L, on polycrystalline Cu surfaces in alkaline electrolytes is known to be responsible for CORR activities, while CO adsorbed on bridge sites are not.¹⁹ The SEIRAS spectrum of the CO_L band on Cu in 0.1 M KOH with a stirring rate of 800 rpm shows the main band centered at 2069 cm⁻¹ with a shoulder at 2081 cm⁻¹ (blue trace in Figure 1a), attributable to CO adsorbed on the terrace and step sites, respectively.^{20–22} There is no peak for solution phase CO detectable because of its low solubility in aqueous solutions (Figure S2). A ~70% drop in the intensity of the CO_I band is observed when the stirring is turned off. Moreover, the shoulder corresponding to CO adsorbed on step sites completely disappears. The drastic decrease in the intensity of the CO_L band without stirring, as compared to the stirred case, indicates a precipitous drop in the surface CO coverage. This could be attributed to the slow mass transport of dissolved CO to the surface, as adsorbed CO is consumed in the CORR. We note that literature shows detectable current densities toward CORR products at potentials below -0.45 V on polycrystalline Cu in CO-saturated 0.1 M KOH electrolyte. The disappearance of the CO_L band on step sites without stirring indicate that adsorbed CO on these sites are preferentially consumed in CORR (i.e., step sites are more active than terrace sites on Cu in CORR, which is consistent with literature).^{4,23} Similar measurements are conducted at −0.7 V (Figure 1b). While CO_L bands corresponding to CO adsorbed on terrace and step sites are observed when stirring, no clear CO_L band appears without stirring. This contrast highlights the importance of including forced convection in the design of operando spectroscopic cells, as the lack of CO_L

band at -0.7 V could be mistakenly interpreted as lack of adsorbed CO during the CORR in reactivity studies at this potential. We note that the need for forced convection in electrocatalytic systems is well recognized, 9,24 and thus, the impact of stirring on spectroscopic observations, manifested in the CORR in this work, is expected to be universal.

With the stirred SEIRAS cell, stirring rates beyond 300 rpm do not appear to have any appreciable impact on the spectroscopic observations. SEIRAS experiments with four stirring rates (i.e., 0, 300, 800, and 1300 rpm) are conducted on Cu in CO-saturated 0.1 M KOH at -0.6 V. The intensity of the CO_L band with a stirring rate of 800 rpm decreases gradually with time (Figure S3a), which is attributed to surface reconstruction of the Cu surface at this condition. Reconstruction of the polycrystalline Cu surface at typical CO₂RR and CORR conditions has been reported in the literature and our previous work. The integrated area of the CO_L band vs time is plotted as a baseline in Figure 2 (black symbols and trace) by normalizing to the intensity at the beginning (to account for the variability of absolute intensities among individual SEIRAS experiments). In a separate experiment, SEIRA spectra are collected at -0.6 V in COsaturated 0.1 M KOH with the stirring rate decreasing every 2 min starting at 1300 rpm, to 800 rpm, 300 rpm, and finally 0 rpm. The integrated area of the CO_L band is also plotted vs time by normalizing to the initial intensity (Figure 2). The traces collected at different stirring rates almost overlap with the baseline at stirring rates equal to or greater than 300 rpm but are significantly lower without stirring. A similar result is obtained when the stirring rate is increased from 300 to 1300 rpm (Figure S3b), indicating that stirring rates beyond 300 rpm do not provide additional benefits. All further stirred experiments are conducted at a stirring rate of 800 rpm. The observed lack of change in CO concentration at the surface with stirring rates above 300 rpm is consistent with two simple mass transport models detailed in the Supporting Information section (Figures S6-S17).

Following the CO_L peak area in different electrolytes and at different potentials provides insights into the effect of cations

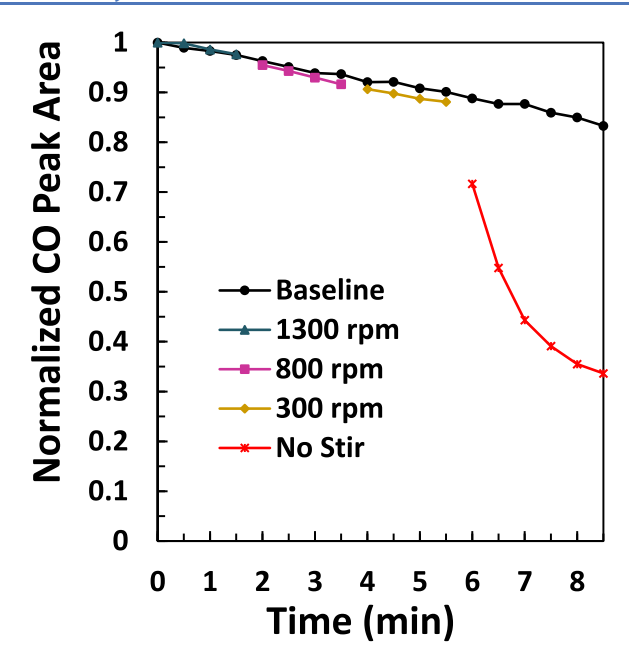


Figure 2. Tracking the linearly bonded CO peak area (normalized to the peak area at the first data point at minute 0) with time at different stirring rates in CO-saturated 0.1 M KOH at -0.6 V on a chemically deposited polycrystalline Cu film. Baseline is also collected at -0.6 V in CO-saturated 0.1 M KOH.

and potential on the CORR. Similar to the investigations at various stirring rates, a trace of the normalized integrated area of the CO₁ band vs time is first collected in 0.1 M KOH at -0.7 V with stirring to serve as the baseline to account for the gradual reduction in CO_I band intensity with time due to surface reconstruction (black trace in Figure 3a). In 0.1 M LiOH at -0.4 V, the area of the CO_L band over time is barely impacted by turning stirring off after 2 min and back on after 5 min, as evidenced by its extensive overlap with the baseline (Figure 3a). This is expected as no detectable CORR occurs at -0.4 V, 4,10,16 and thus, the surface CO coverage should be independent of stirring. The slight increase in the peak area right after the resumption of stirring could be attributed to the coalescing and desorption of bubbles formed via HER facilitated by stirring. Conducting similar experiments in 0.1 M LiOH at -0.6 and -0.7 V show minor but increasing reduction in the area of the CO_L band when the stirring is switched off. This is consistent with increasing CORR rate when stepping from -0.6 to -0.7 V in 0.1 M LiOH previously reported by the Koper group. 16 A 22% and 39% drop in peak area is observed at -0.6 and -0.7 V in LiOH when stopping stirring, respectively, suggesting the reduction in CO coverage without stirring. It is noteworthy that the traces obtained at -0.6 and -0.7 V quickly recover to the baseline upon resuming stirring, further suggesting that the steady-state CO surface coverage in LiOH relative to its initial coverage with stirring is similar to that in KOH despite the higher CORR activity in KOH.¹⁶ This is an indication that the mass transport of CO is able to keep up with its consumption in the CORR with stirring. In contrast, more drastic reductions in the CO_L band by ~70% and 90% occur when similar experiments are conducted in 0.1 M KOH at -0.6 and -0.7 V, respectively, determined from the spectra presented in Figure 1. Upon resumption of stirring, the CO peak intensity recovers at -0.6and -0.7 V in KOH to a steady state within 2 min; however, it is 16% and 44% lower than the baseline, respectively. These

observations show that the lack of stirring in KOH promotes the reconstruction and deactivation of the polycrystalline Cu surface, while this effect is negligible in LiOH. At -0.4 and −0.6 V in both LiOH and KOH, when stirring is stopped after 2 min, the current decreases concurrently, which quickly recovers when the stirring is resumed (Figure 3b,c). This has been attributed to the enhanced rate of bubbles coalescing, and desorption due to stirring.²⁷ A similar stirring-dependent current response is observed at -0.7 V in KOH; however, the effect of stirring on the current is diminished as compared with the cases at -0.4 and -0.6 V. This is likely because bubble formation is already quite facile in KOH at -0.7 V at a steadystate current density of ~1.9 mA/cm² (Figure 3c). In contrast, the current increases slightly in LiOH at -0.7 V upon stopping stirring (Figure 3b). This could be rationalized by the reduced CO coverage at this potential (Figure 3a), which opens up sites for the competing hydrogen evolution reaction (HER), 28,29 the dominant reaction in Li-based electrolytes at the potential range investigated based on previous studies by the Bell and Koper groups. 16,30 The Bell group reported a 3-4-fold higher HER current density compared with CORR at -0.8 V in COsaturated 0.1 M LiHCO₃ solutions.³⁰ From the perspective of the HER, the surface is almost completely poisoned by the unreactive adsorbed CO at -0.4 and -0.6 V in LiOH, resulting in the low current densities compared with those in KOH.

Reactivity results of CORR in KOH at -0.7 V with and without stirring provide insights into the impact of surface CO coverage on product distributions and the distribution of adsorbed CO on the surface. Since the surface CO coverage decreases by approximately an order of magnitude in KOH at -0.7 V upon stopping stirring (Figures 1b and 3a), reactions conducted with and without stirring could reveal the impact of CO coverage on the reactivity. The Faradaic efficiency (FE) for HER increases from 64% when stirred to 78% without stirring (Figure 4a), which is expected as more surface sites are available for the competing HER when the CO supply is limited by its mass transport without forced convection. Importantly, the relative selectivities for different CORR products are not impacted by the drastically different CO coverages (Figure 4b). This is unexcepted because a lower CO coverage should lead to lower selectivity for C-C coupling products given that there is a consensus in the literature that the rate-limiting step of C-C coupling in the CORR is the coupling of two surface adsorbed CO molecules, supported by the lack of pH dependence in the formation rates of C–C coupled products. The only reasonable explanation for these observations is that adsorbed CO molecules are not evenly distributed on the Cu surface. Instead, it is likely that adsorbed CO exists in patches so that a lower overall CO coverage leads to a lower density of these patches, rather than a decrease in the average probability of an adsorbed CO finding an adjacent CO to couple with (Figure 4c). Previous studies have reported a change in product distribution (from C₂₊ to C₁ products) under mass transport limitation conditions induced by higher overpotentials.^{3,34} However, it is unclear whether this change is caused by the electrode potential, the CO coverage, or a combination of both. In contrast, changing the surface CO coverage by controlling the forced convection could isolate the impact of CO coverage on the product distribution. Other reports have shown that a decrease in partial pressure of CO or CO₂ shows a decrease in the rate of formation of all CORR or CO_2RR products $(C_1 \text{ and } C_{2+})$

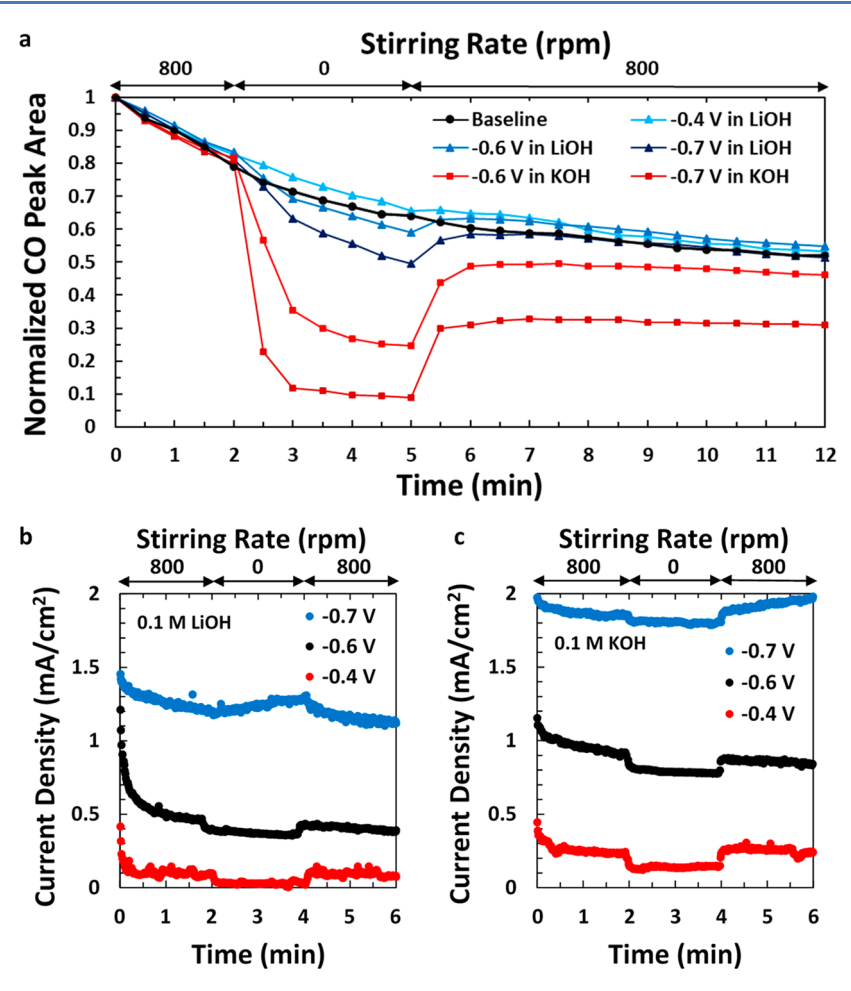


Figure 3. (a) Tracking the linearly bonded CO peak area (normalized to the peak area at the first data point at minute 0) with time at each potential to highlight the impact of stirring on CO coverage at CORR potentials on a chemically deposited polycrystalline Cu film. Baseline is collected at -0.7 V in CO-saturated 0.1 M KOH. (b) Current profiles (absolute value) at different potentials on polycrystalline Cu foils highlighting the impact of stirring on the rate of reaction in CO-saturated 0.1 M LiOH and (c) 0.1 M KOH solutions.

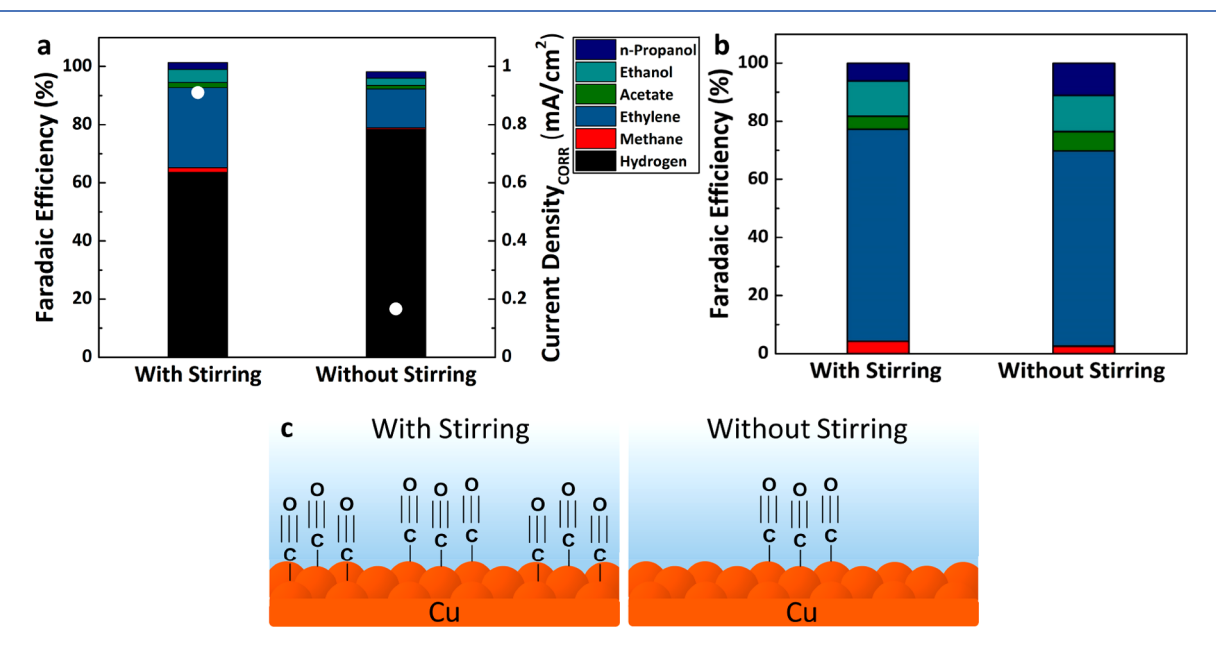


Figure 4. (a) Faradaic efficiency of products formed along with the CORR current density with and without stirring on polycrystalline Cu foil electrodes at -0.7 V in CO-saturated 0.1 M KOH. (b) Faradaic efficiency of CORR products in panel (a) renormalized after omitting the hydrogen Faradaic efficiency. (c) Schematic of the change in CO surface coverage when stirring is stopped at ≤ -0.6 V on a polycrystalline Cu electrode in CO-saturated 0.1 M KOH.

respectively, 4,35 which is consistent with our results. The lack of peak shift when the CO coverage decreases by ~70% upon stopping stirring at -0.6 V in KOH (Figure 1a) indicates that the average distance among adsorbed CO molecules does not change substantially. This is consistent with the hypothesis that adsorbed CO on Cu exist in patches, though it must be noted that these shifts in peak position with CO coverage on Cu are usually small (<10 cm⁻¹) and may not be detected.⁶ Another possible cause for the rapid decrease in CO on step site's peak intensity vs the terrace site's intensity (Figure 1a) is the intensity borrowing of the higher-wavenumber band (step site) at the expense of the lower-wavenumber band (terrace site).21 Borguet and co-workers showed that the rate of decrease of CO on step and terrace sites with decreasing coverage was similar except at high CO coverages.²² It is unlikely for the band corresponding to the step sites to disappear preferentially as the surface CO coverage decreases solely because of the lack of the dipole coupling (Figure S4). Thus, we conclude that under mass transport limitation conditions, the rapid decrease of CO on step sites is due to the increased CORR activity and not due to a change in the proximity of adjacent CO molecules. Previous studies have mentioned coadsorbed hydroxide could impact the CO coverage, 11 but we note that no appreciable difference is observed in the OH stretching or bending modes with and without stirring (Figure S5), suggesting no detectable level of change in surface coverage of adsorbed OH (if any) affecting our interpretation.

In conclusion, this work demonstrates the impact of mass transport limitations on the CO coverage at reaction potentials and the need for spectroscopic techniques with forced convection to produce reliable insights to construct reaction mechanisms. CO mass transport limitations reduce the overall CO coverage on the Cu surface which promotes HER at the expense of the CORR. The remaining CO adsorbs in patches such that the local density of adsorbed CO is relatively independent of the overall CO coverage, which explains the lack of dependence of selectivity for various CORR products on the overall surface CO coverage.

ASSOCIATED CONTENT

S Supporting Information

The Supporting Information is available free of charge at https://pubs.acs.org/doi/10.1021/acscatal.9b03581.

Additional content including detailed experimental methods, spectro-electrochemical cell sketch, supplementary ATR-SEIRAS spectra, CO peak area data, boundary layer calculations, and surface CO concentration modeling results (PDF)

AUTHOR INFORMATION

Corresponding Authors

*E-mail: bxu@udel.edu.

*E-mail: luqicheme@mail.tsinghua.edu.cn.

ORCID

Jing Li: 0000-0001-7538-246X Qi Lu: 0000-0002-0380-2629 Bingjun Xu: 0000-0002-2303-257X

Notes

The authors declare no competing financial interest.

ACKNOWLEDGMENTS

A.M., J.A., and B.X. acknowledge the support of the National Science Foundation CAREER Program (Award No. CBET-1651625). J.L. and Q.L. acknowledge the National Natural Science Foundation of China (grant number 21872079, 21606142). The authors also thank the University of Delaware College of Engineering Machine Shop for the fabrication of custom spectro-electrochemical cells.

REFERENCES

- (1) Hori, Y.; Takahashi, R.; Yoshinami, Y.; Murata, A. Electrochemical Reduction of CO at a Copper Electrode. *J. Phys. Chem. B* **1997**, *101*, 7075–7081.
- (2) Wuttig, A.; Liu, C.; Peng, Q.; Yaguchi, M.; Hendon, C. H.; Motobayashi, K.; Ye, S.; Osawa, M.; Surendranath, Y. Tracking a Common Surface-Bound Intermediate during CO₂-to-Fuels Catalysis. *ACS Cent. Sci.* **2016**, *2*, 522–528.
- (3) Li, J.; Chang, K.; Zhang, H.; He, M.; Goddard, W. A.; Chen, J. G.; Cheng, M.-J.; Lu, Q. Effectively Increased Efficiency for Electroreduction of Carbon Monoxide Using Supported Polycrystal-line Copper Powder Electrocatalysts. *ACS Catal.* **2019**, *9*, 4709–4718.
- (4) Wang, L.; Nitopi, S. A.; Bertheussen, E.; Orazov, M.; Morales-Guio, C. G.; Liu, X.; Higgins, D. C.; Chan, K.; Nørskov, J. K.; Hahn, C.; Jaramillo, T. F. Electrochemical Carbon Monoxide Reduction on Polycrystalline Copper: Effects of Potential, Pressure, and pH on Selectivity toward Multicarbon and Oxygenated Products. *ACS Catal.* **2018**, *8*, 7445–7454.
- (5) Kunimatsu, K. Infrared Spectroscopic Study of Methanol and Formic Acid Adsorbates on a Platinum Electrode. Part I. Comparison of the Infrared Absorption Intensities of Linear CO_(a) Derived from CO, CH₃OH and HCOOH. *J. Electroanal. Chem. Interfacial Electrochem.* **1986**, 213, 149–157.
- (6) Woodruff, D. P.; Hayden, B. E.; Prince, K.; Bradshaw, A. M. Dipole Coupling and Chemical Shifts in IRAS of CO Adsorbed on Cu(110). Surf. Sci. 1982, 123, 397–412.
- (7) Samjeské, G.; Komatsu, K. I.; Osawa, M. Dynamics of CO Oxidation on a Polycrystalline Platinum Electrode: A Time-Resolved Infrared Study. *J. Phys. Chem. C* **2009**, *113*, 10222–10228.
- (8) Dunwell, M.; Wang, J.; Yan, Y.; Xu, B. Surface Enhanced Spectroscopic Investigations of Adsorption of Cations on Electrochemical Interfaces. *Phys. Chem. Chem. Phys.* **2017**, *19*, 971–975.
- (9) Dunwell, M.; Yang, X.; Setzler, B. P.; Anibal, J.; Yan, Y.; Xu, B. Examination of Near-Electrode Concentration Gradients and Kinetic Impacts on the Electrochemical Reduction of CO₂ Using Surface-Enhanced Infrared Spectroscopy. ACS Catal. 2018, 8, 3999–4008.
- (10) Malkani, A.; Dunwell, M.; Xu, B. Operando Spectroscopic Investigations of Copper and Oxide-Derived Copper Catalysts for Electrochemical CO Reduction. *ACS Catal.* **2019**, *9*, 474–478.
- (11) Iijima, G.; Inomata, T.; Yamaguchi, H.; Ito, M.; Masuda, H. Role of a Hydroxide Layer on Cu Electrodes in Electrochemical CO₂ Reduction. *ACS Catal.* **2019**, *9*, 6305–6319.
- (12) Osawa, M.; Ikeda, M. Surface-Enhanced Infrared-Absorption of Para-Nitrobenzoic Acid Deposited on Silver Island Films- Contributions of Electromagnetic and Chemical Mechanisms. *J. Phys. Chem.* **1991**, *95*, 9914–9919.
- (13) Osawa, M. Surface-Enhanced Infrared Absorption. *Top. Appl. Phys.* **2001**, *81*, 163–187.
- (14) Osawa, M.; Ataka, K.; Yoshii, K.; Yotsuyanagi, T. Surface-Enhanced Infrared ATR Spectroscopy for in Situ Studies of Electrode/Electrolyte Interfaces. *J. Electron Spectrosc. Relat. Phenom.* **1993**, *64–65*, 371–379.
- (15) Pérez-Gallent, E.; Figueiredo, M. C.; Calle-Vallejo, F.; Koper, M. T. M. Spectroscopic Observation of a Hydrogenated CO Dimer Intermediate During CO Reduction on Cu(100) Electrodes. *Angew. Chem., Int. Ed.* **2017**, *56*, 3621–3624.
- (16) Pérez-Gallent, E.; Marcandalli, G.; Figueiredo, M. C.; Calle-Vallejo, F.; Koper, M. T. M. Structure- and Potential-Dependent

Cation Effects on CO Reduction at Copper Single-Crystal Electrodes. *J. Am. Chem. Soc.* **2017**, *139*, 16412–16419.

- (17) Chen, Y. X.; Heinen, M.; Jusys, Z.; Behm, R. J. Kinetics and Mechanism of the Electrooxidation of Formic Acid-Spectroelectrochemical Studies in a Flow Cell. *Angew. Chem., Int. Ed.* **2006**, 45, 981–985.
- (18) Nakamura, M.; Shibutani, K.; Hoshi, N. In-Situ Flow-Cell IRAS Observation of Intermediates during Methanol Oxidation on Low-Index Platinum Surfaces. *ChemPhysChem* **2007**, *8*, 1846–1849.
- (19) Gunathunge, C. M.; Ovalle, V. J.; Li, Y.; Janik, M. J.; Waegele, M. M. Existence of an Electrochemically Inert CO Population on Cu Electrodes in Alkaline pH. ACS Catal. 2018, 8, 7507–7516.
- (20) Hollins, P.; Davies, K. J.; Pritchard, J. Infrared Spectra of CO Chemisorbed on a Surface Vicinal to Cu(110): The Influence of Defect Sites. *Surf. Sci.* **1984**, *138*, 75–83.
- (21) Hollins, P. The Influence of Surface Defects on the Infrared Spectra of Adsorbed Species. Surf. Sci. Rep. 1992, 16, 51–94.
- (22) Borguet, E.; Dai, H. L. Site-Specific Properties and Dynamical Dipole Coupling of CO Molecules Adsorbed on a Vicinal Cu(100) Surface. *J. Chem. Phys.* **1994**, *101*, 9080–9095.
- (23) Liu, X.; Xiao, J.; Peng, H.; Hong, X.; Chan, K.; Nørskov, J. K. Understanding Trends in Electrochemical Carbon Dioxide Reduction Rates. *Nat. Commun.* **2017**, *8*, 15438.
- (24) Raciti, D.; Mao, M.; Wang, C. Mass Transport Modelling for the Electroreduction of CO₂ on Cu Nanowires. *Nanotechnology* **2018**, 29, 044001.
- (25) Gunathunge, C. M.; Li, X.; Li, J.; Hicks, R. P.; Ovalle, V. J.; Waegele, M. M. Spectroscopic Observation of Reversible Surface Reconstruction of Copper Electrodes under CO₂ Reduction. *J. Phys. Chem. C* 2017, 121, 12337–12344.
- (26) Kim, Y. G.; Baricuatro, J. H.; Javier, A.; Gregoire, J. M.; Soriaga, M. P. The Evolution of the Polycrystalline Copper Surface, First to Cu(111) and Then to Cu(100), at a Fixed CO₂RR Potential: A Study by Operando EC-STM. *Langmuir* **2014**, *30*, 15053–15056.
- (27) Gabrielli, C.; Huet, F.; Nogueira, R. P. Electrochemical Impedance of H₂-Evolving Pt Electrode under Bubble-Induced and Forced Convections in Alkaline Solutions. *Electrochim. Acta* **2002**, 47, 2043–2048.
- (28) Schreier, M.; Yoon, Y.; Jackson, M. N.; Surendranath, Y. Competition between H and CO for Active Sites Governs Copper-Mediated Electrosynthesis of Hydrocarbon Fuels. *Angew. Chem., Int. Ed.* **2018**, *57*, 10221–10225.
- (29) Ooka, H.; Figueiredo, M. C.; Koper, M. T. M. Competition between Hydrogen Evolution and Carbon Dioxide Reduction on Copper Electrodes in Mildly Acidic Media. *Langmuir* **2017**, 33, 9307–9313.
- (30) Resasco, J.; Chen, L. D.; Clark, E.; Tsai, C.; Hahn, C.; Jaramillo, T. F.; Chan, K.; Bell, A. T. Promoter Effects of Alkali Metal Cations on the Electrochemical Reduction of Carbon Dioxide. *J. Am. Chem. Soc.* **2017**, *139*, 11277–11287.
- (31) Cheng, T.; Xiao, H.; Goddard, W. A. Full Atomistic Reaction Mechanism with Kinetics for CO Reduction on Cu(100) from Ab Initio Molecular Dynamics Free-Energy Calculations at 298 K. *Proc. Natl. Acad. Sci. U. S. A.* **2017**, *114*, 1795–1800.
- (32) Montoya, J. H.; Shi, C.; Chan, K.; Nørskov, J. K. Theoretical Insights into a CO Dimerization Mechanism in CO₂ Electroreduction. *J. Phys. Chem. Lett.* **2015**, *6*, 2032–2037.
- (33) Calle-Vallejo, F.; Koper, M. T. M. Theoretical Considerations on the Electroreduction of CO to C_2 Species on Cu(100) Electrodes. *Angew. Chem., Int. Ed.* **2013**, 52, 7282–7285.
- (34) Nitopi, S.; Bertheussen, E.; Scott, S. B.; Liu, X.; Engstfeld, A. K.; Horch, S.; Seger, B.; Stephens, I. E. L.; Chan, K.; Hahn, C.; Nørskov, J. K.; Jaramillo, T. F.; Chorkendorff, I. Progress and Perspectives of Electrochemical CO₂ Reduction on Copper in Aqueous Electrolyte. *Chem. Rev.* **2019**, *119*, 7610–7672.
- (35) Kyriacou, G. Z.; Anagnostopoulos, A. K. Influence of CO₂ Partial Pressure and the Supporting Electrolyte Cation on the Product Distribution in CO₂ Electroreduction. *J. Appl. Electrochem.* **1993**, 23, 483–486.